# Calculation of the energy-level structure of the HfF$^+$ cation to search for parity-nonconservation effects

I. P. Kurchavov ◉[*] and A. N. Petrov[†]

*National Research Centre "Kurchatov Institute," B. P. Konstantinov Petersburg Nuclear Physics Institute,*
*Gatchina, Leningrad District 188300, Russia*
*and Saint Petersburg State University, 7/9 Universitetskaya Emb., Saint Petersburg 199034, Russia*

The energy shifts due to interactions violating time-reversal invariance and parity symmetry, $g$ factors, and energies for the hyperfine levels of the ground rotational level of the $^3\Delta_1$ electronic state of the $^{177}$Hf $^{19}$F$^+$ ion are calculated as functions of the external electric and magnetic fields. The calculations can be used to plan an experiment to measure the magnetic quadrupole moment of the $^{177}$Hf nucleus and to interpret the obtained data.

## I. INTRODUCTION

The current limit for the electron electric dipole moment (eEDM) with cation $^{180}$HfF$^+$ $|d_e| < 1.3 \times 10^{-28}$ $e$ cm (90% confidence) was obtained using trapped $^{180}$Hf $^{19}$F$^+$ ions [1] with a spinless $^{180}$Hf isotope. The measurements were performed on the ground rotational, $J=1$, level in the metastable electronic $H\,^3\Delta_1$ state. Considering the great potential for investigations of time ($\mathcal{T}$) and parity ($\mathcal{P}$) violating effects in HfF$^+$, it was proposed in Ref. [2] to use $^{177}$Hf $^{19}$F$^+$ and $^{179}$Hf $^{19}$F$^+$ ions to measure the nuclear magnetic quadrupole moment (MQM) of $^{177}$Hf and $^{179}$Hf nuclei which have spins $I = 7/2$ and $9/2$, respectively.

The $\mathcal{T}$- and $\mathcal{P}$-odd effects arising from the MQM, eEDM, and scalar–pseudoscalar nucleus–electron neutral current (SP) interaction in $^{177}$Hf $^{19}$F$^+$ and in $^{177}$Hf $^{19}$F$^+$ were considered in previous work [3]. The role of hyperfine interaction was investigated. The MQM shift as a function of external static electric field was calculated and it was shown that MQM effects can be distinguished from the electron EDM due to the implicit dependence of MQM shift on the hyperfine sublevel. The MQM effect was expressed in terms of proton EDM, QCD vacuum angle $\theta$, and quark chromo-EDMs. It was confirmed that measurement of the nuclear MQM is promising for establishing new restrictions on these properties.

The important characteristic of the experiments on HfF$^+$ is that *rotating* magnetic and electric fields are used to trap ions. In this case, the magnetic field, in contrast to experiments in static fields, is not an auxiliary tool, but should ensure a nonzero energy shift due to possible $\mathcal{T}$- and $\mathcal{P}$-odd effects [1,4]. To completely polarize the molecule and to access the maximum $\mathcal{T}$- and $\mathcal{P}$-odd effect both rotating electric and magnetic fields should be large enough. The saturating value of the magnetic field strongly depends on the considered Zeeman sublevel of the ion. These values are required to plan the experiment and their calculation is the main aim of the paper. For this purpose the sensitivity of Zeeman sublevels of different hyperfine components of the ground rotational level of the $^3\Delta_1$ state in $^{177}$HfF$^+$ to $\mathcal{T}$- and $\mathcal{P}$-odd properties in external variable electric and magnetic fields was calculated.

To populate the required levels in experiments one needs to know the energy-level structure. This problem is especially important for $^{177}$HfF$^+$ since it has a dense spectrum due to the high nuclear spin of $^{177}$Hf. Further, the knowledge of $g$ factors helps to control and suppress systematic effects due to stray magnetic field [5,6]. Therefore calculations of these properties in external fields are also made in our paper.

## II. METHODS

We present the molecular Hamiltonian in the external fields for $^{177}$Hf $^{19}$F$^+$ as

$$\hat{\mathbf{H}}_{mol} = \hat{\mathbf{H}}_{el} + \hat{\mathbf{H}}_{rot} + \hat{\mathbf{H}}_{hfs} + \hat{\mathbf{H}}_{ext}, \quad (1)$$

where $\hat{\mathbf{H}}_{el}$ is the electronic Hamiltonian,

$$\hat{\mathbf{H}}_{rot} = B_{rot}\mathbf{J}^2 - 2B_{rot}(\mathbf{J} \cdot \mathbf{J}^e) \quad (2)$$

is rotational interaction, $B_{rot} = 0.2989$ cm$^{-1}$ [7] is the rotational constant, $\mathbf{J}$ is total molecular angular momentum minus nuclear spins, $\mathbf{J}^e$ is total angular momentum of the electronic subsystem,

$$
\begin{aligned}
\hat{\mathbf{H}}_{hfs} = {} & g_F \mu_N I^2 \times \sum_i \left( \frac{\boldsymbol{\alpha}_i \times \boldsymbol{r}_{2i}}{r_{2i}^3} \right) \\
& + g_{Hf}\mu_N I^1 \times \sum_i \left( \frac{\boldsymbol{\alpha}_i \times \boldsymbol{r}_{1i}}{r_{1i}^3} \right) \\
& - e^2 \sum_q (-1)^q \hat{Q}_q^2(I^1) \sum_i \sqrt{\frac{2\pi}{5}} \frac{Y_{2q}(\theta_{1i},\phi_{1i})}{r_{1i}^3} \quad (3)
\end{aligned}
$$

is hyperfine interaction which includes magnetic hyperfine interaction of electrons with both nuclei and interaction with the electric quadrupole moment of $^{177}$Hf, $g_F = 5.25773$ [8] and $g_{Hf} = 0.2267$ [8] are $^{19}$F and $^{177}$Hf nuclear $g$ factors, $\mu_N$ is the nuclear magneton, $I^1 = 7/2$ is nuclear spin for $^{177}$Hf

─────────
[*]http://www.qchem.pnpi.spb.ru
[†]alexsandernp@gmail.com

and $I^2 = 1/2$ is nuclear spin for $^{19}$F, $\boldsymbol{\alpha}$ is the vector of Dirac matrices, $\boldsymbol{r}_{1i}$ ($\boldsymbol{r}_{2i}$) is the radius vector for the $i$th electron in the coordinate system centered on the Hf(F) nucleus, $\hat{Q}_q^2(I^1)$ is the quadrupole moment operator for the $^{177}$Hf nucleus,

$$\hat{\mathbf{H}}_{\text{ext}} = \mu_B(\mathbf{L}^e - g_s\mathbf{S}^e) \cdot \mathbf{B}$$
$$- g_{\text{F}}\frac{\mu_N}{\mu_B}I^2 \cdot \mathbf{B} - \mathbf{D} \cdot \mathbf{E}$$
$$- g_{\text{Hf}}\frac{\mu_N}{\mu_B}I^1 \cdot \mathbf{B} \qquad (4)$$

describes interaction with external fields, $g_S = -2.0023$ is a free-electron $g$ factor, $\mathbf{D}$ is the dipole moment operator, and $\mu_B$ is the Bohr magneton.

In the present paper we performed two types of calculations: in the presence of static ($\mathbf{E} = \mathbf{E}_{\text{static}}$, $\mathbf{B} = \mathbf{B}_{\text{static}}$) or rotating counterclockwise around the $\hat{z}$ axis [4],

$$\mathbf{E}(t) = \mathcal{E}_{\text{rot}}[\hat{x}\cos(\omega_{\text{rot}}t) + \hat{y}\sin(\omega_{\text{rot}}t)], \qquad (5)$$

$$\mathbf{B}(t) = \mathcal{B}_{\text{rot}}[\hat{x}\cos(\omega_{\text{rot}}t) + \hat{y}\sin(\omega_{\text{rot}}t)], \qquad (6)$$

electric and magnetic fields. Below we set $\omega_{\text{rot}}/2\pi = +250, +150$ kHz as it was in the experiment on $^{180}$Hf $^{19}$F$^+$ ions [1].

Eigenvalues and eigenfunctions are obtained by numerical diagonalization of the molecular Hamiltonian ($\hat{\mathbf{H}}_{\text{mol}}$) over the basis set of the electronic-rotational wave functions:

$$\Psi_\Omega \theta_{M,\Omega}^J(\alpha, \beta)U_{I^1M^1}^{\text{Hf}}U_{I^2M^2}^{\text{F}}. \qquad (7)$$

Here $\Psi_\Omega$ is the electronic wave function; $\theta_{M,\Omega}^J(\alpha, \beta) = \sqrt{(2J+1)/4\pi}D_{M,\Omega}^J(\alpha, \beta, \gamma = 0)$ is the rotational wave function; $\alpha$, $\beta$, and $\gamma$ are Euler angles; $U_{I^1M^1}^{\text{Hf}}$ and $U_{I^2M^2}^{\text{F}}$ are the Hf and F nuclear spin wave functions; $M$ ($\Omega$) is the projection of the molecule angular momentum on the laboratory $\hat{z}$ (internuclear $\zeta$) axis; and $M^{1,2}$ are the projections of the nuclear angular momenta on the same axis.

The low-lying electronic basis states $^3\Delta_1$, $^3\Delta_2$, $^3\Pi_{0^+}$, and $^3\Pi_{0^-}$ were included to calculations. Our primary interest is the $^3\Delta_1$ state and therefore only the hyperfine interaction for this state is considered. As is shown previously in Ref. [6], taking into account nonadiabatic interactions with $^3\Delta_2$, $^3\Pi_{0^+}$, and $^3\Pi_{0^-}$ is important for accurate evaluation of $g$ factors and other related properties of $^3\Delta_1$.

Following Ref. [4], calculations for the interaction with rotating fields are performed by transition to the rotating frame. Electronic matrix elements required for evaluation of $\hat{\mathbf{H}}_{\text{mol}}$ on the basis set (7) are taken from Refs. [3,6].

## III. RESULTS

The hyperfine structure of the ground rotational level $J = 1$ of the $^3\Delta_1$ state calculated with the field-free Hamiltonian is shown in Fig. 1. The presented levels are well described by the coupling scheme:

$$\mathbf{F_1} = \mathbf{J} + \mathbf{I^1},$$
$$\mathbf{F} = \mathbf{F_1} + \mathbf{I^2}. \qquad (8)$$

For $J = 1$, $^3\Delta_1$ $^{177}$Hf F$^+$ we have $F_1 = 5/2, 7/2, 9/2$. Hyperfine interaction with the fluorine nucleus further splits
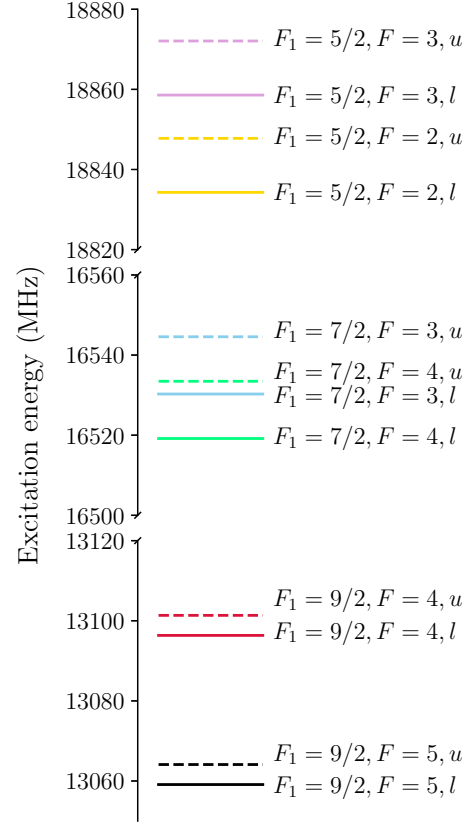


FIG. 1. $^3\Delta_1$ $J = 1$ level scheme of $^{177}$Hf $^{19}$F$^+$ including the $\Omega$ (projection of the total moment on the internuclear axis) doubling that occurs due to the rotation of the molecule. Here the dashed line is for the upper $\Omega$ doublet and the solid line is for the lower doubling.

energy levels with total momentum $F = F_1 \pm 1/2$. Figure 1 also depict $\Omega$ doublets with opposite parity ($\Omega = \pm 1$) caused by rotation of molecule and electric quadrupole hyperfine interaction.

$g$ factors for the field-free case and in the presence of an external static electric field were calculated by finite field method [9,10]. We define the $g$ factors such that the Zeeman shift is equal to [6,11]

$$E_{\text{Zeeman}} = -g(E_{\text{static}})\mu_B B_{\text{static}}m_F, \qquad (9)$$

where $m_F$ is the projection of the total angular momentum on the laboratory $\hat{z}$ axis. The simple analytical formula for the $g$ factor for zero electric field according to the coupling scheme (8) reads

$$g = g^1 \frac{F(F+1) + F_1(F_1+1) - I^2(I^2+1)}{2F_1(F_1+1)J(J+1)}$$
$$+ g_{\text{F}}\frac{\mu_N}{\mu_B}\frac{F(F+1) - F_1(F_1+1) + I^2(I^2+1)}{2F(F+1)}, \qquad (10)$$

where

$$g^1 = -G_\parallel \frac{F_1(F_1+1) + J(J+1) - I^1(I^1+1)}{2F_1(F_1+1)J(J+1)} +$$
$$+ g_{\text{Hf}}\frac{\mu_N}{\mu_B}\frac{F_1(F_1+1) - J(J+1) + I^1(I^1+1)}{2F_1(F_1+1)}. \qquad (11)$$

TABLE I. Values of $g$ factors for the $^3\Delta_1$ $J = 1$ level obtained by various approaches for the field-free case. Here $[n]$ stands for $\times 10^n$.

| $F_1$ | $F$ | $g$[a] | $g$[b] | $\delta g(\%)$ | $g$[c] |
|-------|-----|--------|--------|----------------|--------|
| 5/2 | 3 | 2.01[−3] | 1.93[−3] | −4 | 1.883[−3] |
|     | 2 | 1.67[−3] | 1.55[−3] | −7 | 1.484[−3] |
| 7/2 | 3 | −6.48[−4] | −8.3[−4] | −28 | −8.458[−4] |
|     | 4 | 1.32[−4] | −2.94[−6] |  | −1.591[−5] |
| 9/2 | 4 | −1.62[−3] | −1.76[−3] | −9 | −1.743[−3] |
|     | 5 | −8.04[−4] | −9.18[−4] | −14 | −9.043[−4] |

[a]Eq. (10).

[b]Numerical calculation.

[c]Numerical calculation; nonadiabatic interaction between different electronic states is neglected.

Here $\mu_N$ is the nuclear magneton, and $g_{Hf}$ and $g_F$ are $^{177}$Hf and $^{19}$F nuclear $g$ factors. $G_{\|}$ is the matrix element that is responsible for the electronic contribution:

$$G_{\|} = \frac{1}{\Omega}\langle \Psi_{^3\Delta_1}|\hat{L}_\zeta^e - g_s\hat{S}_\zeta^e|\Psi_{^3\Delta_1}\rangle = 0.011\,768. \qquad (12)$$

Equation (10) does not take into account nonadiabatic interaction between different electronic states and hyperfine interaction between different hyperfine sublevels (belonging to the same and different rotational levels). The fourth column of Table I shows the results of numerical calculations (our final value). In numerical calculations we take into account nonadiabatic interaction of $^3\Delta_1$ with $^3\Delta_2$, $^3\Pi_1$ and $^1\Pi_1$ and hyperfine interaction of different rotational states. One can see that numerical calculations differ from values given by
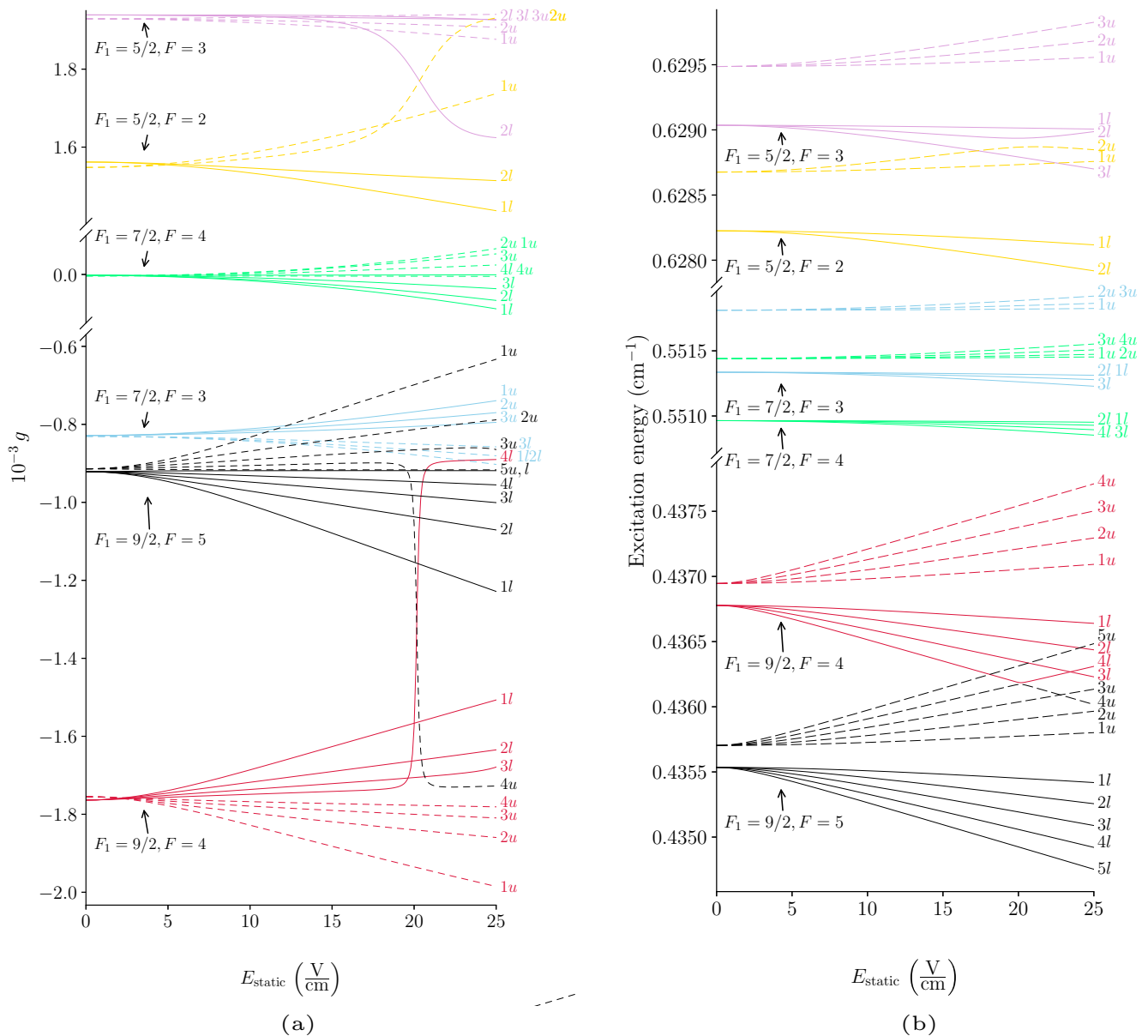


FIG. 2. $g$ factors (a) and energy levels (b) for different projections as functions of the electric field. From the figure we can see that the energy order changes and levels mix when the electric field reaches nearly 20 V/cm. Equality of $g$ factors can reduce systematic errors in experiments.
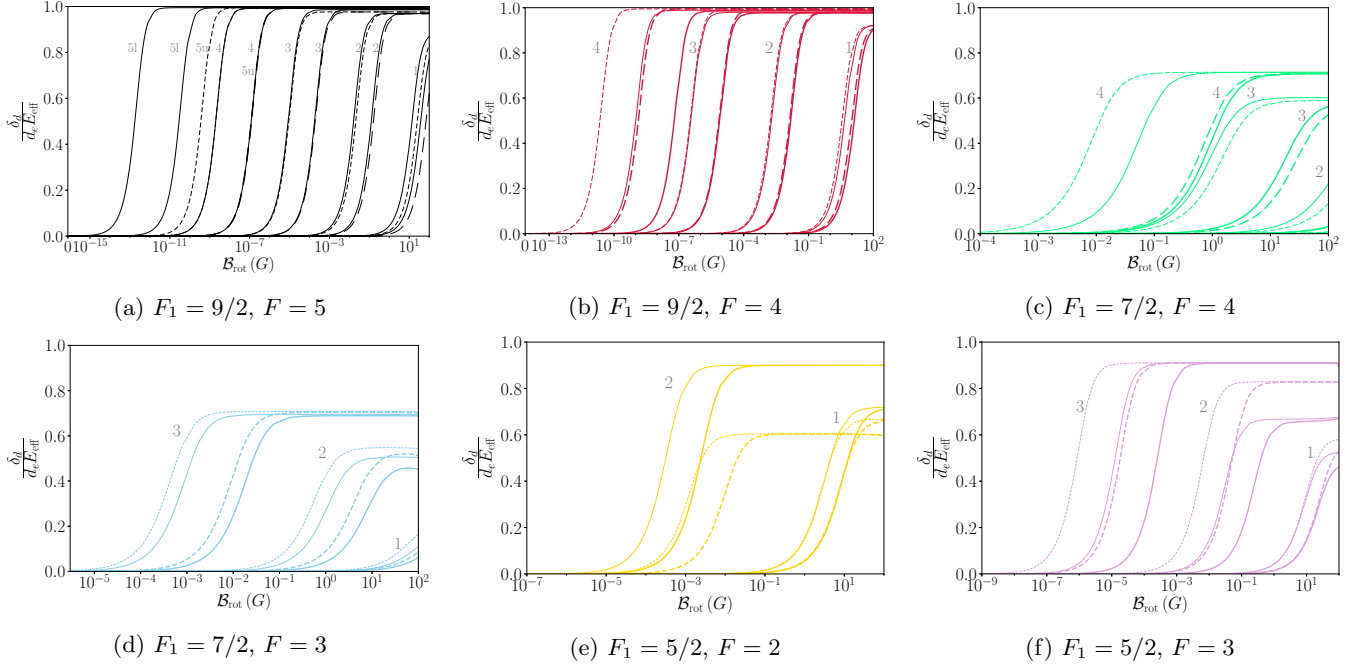
FIG. 3. *e*EDM induced energy shift [4] as a function of the rotating magnetic fields for different projections $m_F$ (gray numbers on the plot). $\mathcal{E}_{\text{rot}} = 24$ V/cm in calculations. The thin line is for $\omega = 150$ kHz and the thick line is for $\omega = 250$ kHz. (a) $F_1 = 9/2$, $F = 5$. (b) $F_1 = 9/2$, $F = 4$. (c) $F_1 = 7/2$, $F = 4$. (d) $F_1 = 7/2$, $F = 3$. (e) $F_1 = 5/2$, $F = 2$. (f) $F_1 = 5/2$, $F = 3$.

Eqs. (10) and (11) by 4–28% except $F_1 = 7/2$ and $F = 4$ where the difference is very large due to near cancellation of different contributions. The relative error for this value can be as large as 100%. In the last column of Table I the results where nonadiabatic interaction is neglected are given. In Fig. 2(a) we present *g* factors for different projections of total momentum $F$ as functions of static electric field. A graph of energy levels in Fig. 2(b) shows that sharp change in *g* factors for $F_1 = 9/2$, $F = 4$, $m_F = 4$; $F_1 = 9/2$, $F = 5$, $m_F = 4$; $F_1 = 5/2$, $F = 2$, $m_F = 2$; and $F_1 = 5/2$, $F = 3$, $m_F = 2$ levels is due to the avoided crossing of their levels and confirms the general statement that levels with the same symmetry cannot intersect. Levels with different projections $m_F$ do not interact and can cross. *g* factors for upper and lower $\Omega$ doublets become equal at $E_{\text{static}} = 2$–6 V/cm for $F_1 = 9/2$, $F = 4$; $F_1 = 7/2$, $F = 4$; and $F_1 = 5/2$, $F = 3$.

One of the main purposes of the paper is to evaluate energy shifts of the Zeeman sublevels due to $\mathcal{T}$- and $\mathcal{P}$-odd electromagnetic interaction of the *e*EDM and nuclear magnetic quadrupole moment with electrons in the external rotating electric and magnetic fields.[1] The energy shifts were calculated as mean values of corresponding $\mathcal{T}$- and $\mathcal{P}$-odd Hamiltonians (see Ref. [3]) with wave functions obtained as described in the previous section. Corresponding calculations for the levels' shifts as functions of rotating magnetic field for rotating electric field $\mathcal{E}_{\text{rot}} = 24$V/cm for different Zeeman sublevels are presented in Figs. 3 and 4. The $m_F = 0$ levels are not sensitive to *e*EDM and MQM and not presented on the

graphs. In case of rotating fields $m_F$ means the projection of the total angular momentum on the direction of the fields. The results are presented in the units of $d_e E_{\text{eff}}$ for *e*EDM shift ($\delta_d$) and $M W_M$ for MQM shift ($\delta_M$) [3], respectively. Here $E_{\text{eff}}$ is the effective electric field given by

$$E_{\text{eff}} = \langle \Psi_{^3\Delta_1} | \sum_i \begin{pmatrix} 0 & 0 \\ 0 & 2\boldsymbol{\sigma}_i \boldsymbol{E}_i \end{pmatrix} | \Psi_{^3\Delta_1} \rangle, \qquad (13)$$

$\boldsymbol{\sigma}$ is the Pauli matrix, $\boldsymbol{E}_i$ is the inner molecular electric field acting on the $i$ electron, and $M$ is the magnetic quadrupole moment of the $^{177}$Hf nucleus:

$$W_M = \frac{3}{2} \frac{1}{\Omega} \langle \Psi_{^3\Delta_1} | \sum_i \left( \frac{\boldsymbol{\alpha}_i \times \mathbf{r}_i}{r_i^5} \right)_\zeta r_\zeta | \Psi_{^3\Delta_1} \rangle. \qquad (14)$$

The values $E_{\text{eff}} = 24$ [12,13], 22.5 [14], and 22.7 GV/cm [15] and $W_M = 0.494 \frac{10^{33}\text{Hz}}{e\,\text{cm}^2}$ [16] have been obtained previously. As one can see from Figs. 3 and 4 the graphs for *e*EDM and MQM are similar and the saturating magnetic field strongly depends on the value of $m_F$. The explanation is as follows. To reach the saturation limit for *e*EDM and MQM shifts, the laboratory electric field $\mathcal{E}_{\text{rot}}$ must be large enough to fully polarize the molecule. Further, the rotating electric field connects the Zeeman sublevels $m_F$ and $-m_F$ and turns the degeneracy between them (in case of static electric field) to a splitting between new eigenstates which are equal-mixed combinations of $m_F$ and $-m_F$. Since $m_F$ and $-m_F$ sublevels have different signs for *e*EDM and MQM shifts, the value for rotating magnetic field, $\mathcal{B}_{\text{rot}}$, has also to be large enough to ensure that $m_F$ becomes a good quantum number and as a result reaches the saturation limit for the levels' shift [4]. The values for calculated splittings described above for upper $\Delta E_u$

---

[1]The dependence of energy shift due to SP interaction is exactly the same as for *e*EDM case [3].
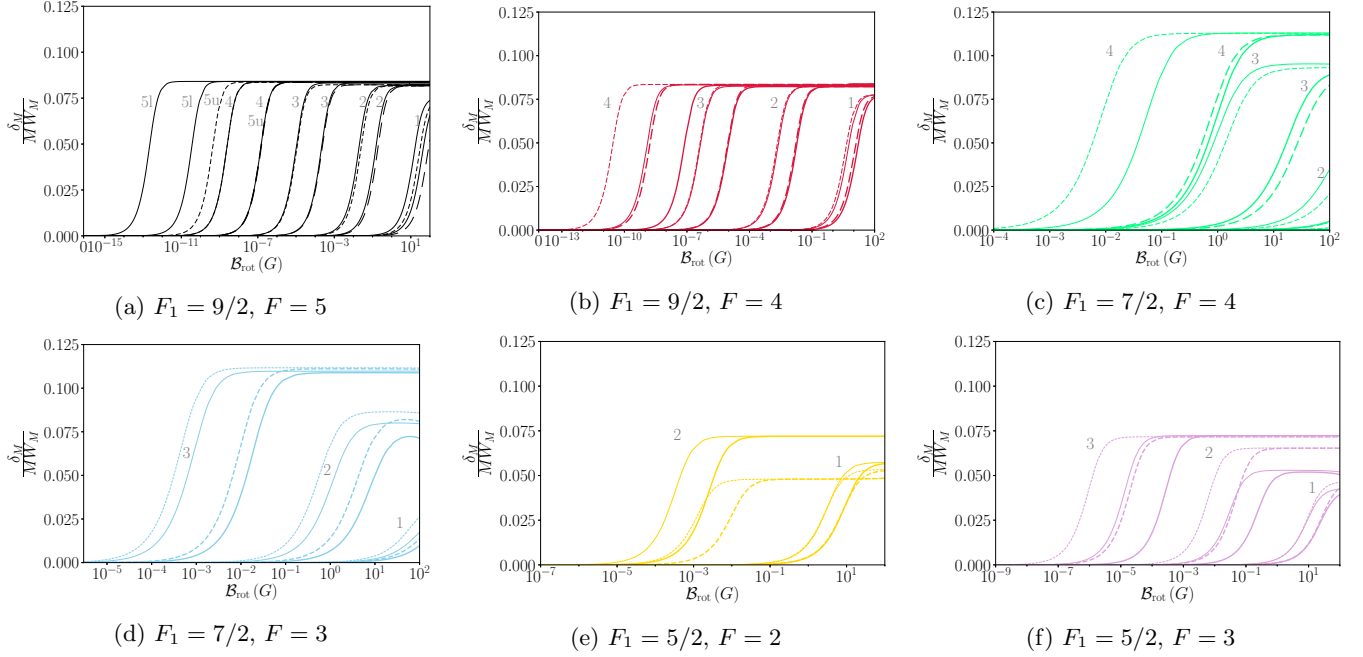
FIG. 4. MQM induced energy shift [4] as a function of the rotating magnetic fields for different projections $m_F$ (gray numbers on the plot). $\mathcal{E}_{\rm rot} = 24$ V/cm in calculations. The thin line is for $\omega = 150$ kHz and the thick line is for $\omega = 250$ kHz. (a) $F_1 = 9/2, F = 5$. (b) $F_1 = 9/2, F = 4$. (c) $F_1 = 7/2, F = 4$. (d) $F_1 = 7/2, F = 3$. (e) $F_1 = 5/2, F = 2$. (f) $F_1 = 5/2, F = 3$.

and lower $\Delta E_l$ $\Omega$ doublets are given in Table II. $\Delta E_{u,l}$ varies widely, by order of magnitude from $10^{-15}$ to $10^{-1}$ MHz. The larger $m_F$ the smaller the splitting [17] expected and smaller $B_{\rm rot}$ needed for saturation. Saturation is not reached for some levels with $m_F = 1, 2$ up to $\mathcal{B}_{\rm rot} = 100$ G.

$J = 1$ $^{180}$HfF$^+$ becomes almost fully polarized for $\mathcal{E}_{\rm rot} > 4$ V/cm [7]. $^{177}$Hf $^{19}$F$^+$ requires a much larger electric field to be polarized due to a larger $\Omega$-doubling effect caused by electric quadrupole hyperfine interaction [3]. For the present calculation we set $\mathcal{E}_{\rm rot} = 24$ V/cm. If required, the calculations can easily be performed for another electric field by the method described in the paper. Note, however, that the electric fields for the experiment should be chosen with caution. It was shown previously that due to the existence of closely spaced levels of $\Omega$ doublets having almost identical properties the experiments on $\Omega = 1$ molecules are very robust against a number of systematic effects related to magnetic fields [5,18] or geometric phases [19,20] and others. However, for some values of electric fields and some states avoided crossings are observed (see Fig. 2). For these points the upper and lower $\Omega$ doublets have different properties (due to large changing of the wave function of one of them involved in avoided crossing) and systematic effects are not suppressed in this case.

Calculations performed in the paper allow one to choose appropriate levels (if any) for the experiment for a given $\mathcal{B}_{\rm rot}$. For example, for parameters $\omega_{\rm rot}/2\pi = +150$ kHz, $\mathcal{E}_{\rm rot} = 24$ V/cm, and $\mathcal{B}_{\rm rot} = 2$G used in the recent experiment [1] the levels $F_1 = 9/2, F = 5, m_F = 2, 3, 4, 5$ and $F_1 = 7/2, F = 4, m_F = 4$ can be considered. According to Figs. 3 and 4 for these levels $\delta_d = 0.99 d_e E_{\rm eff}$, $\delta_M = 0.083 M W_M$ and $\delta_d = 0.71 d_e E_{\rm eff}$, $\delta_M = 0.11 M W_M$, respectively. The levels have large sensitivity and differ-

ent ratio $\delta_d/\delta_M$, which allows us to distinguish $e$EDM and MQM contributions. Instead of $F_1 = 9/2, F = 5, m_F = 2, 3, 4, 5$ and $F_1 = 7/2, F = 4, m_F = 4$ other hyperfine components of fluorine nuclear $F_1 = 9/2, F = 4, m_F = 2, 3, 4$ and $F_1 = 7/2, F = 3, m_F = 3$ which have the same sensitivities can be used.

Hyperfine levels $F_1 = 5/2$ and $9/2$ have about the same sensitivity. In the experiment only one of them can be used. However, using both of them provides an additional opportunity to check the theory and experiment.

## IV. CONCLUSION

Energy levels and $g$ factors as functions of the electric field for the ground rotational level $J = 1$ of the $^3\Delta_1$ electronic state of $^{177}$Hf $^{19}$F$^+$ are calculated, taking into account the hyperfine and nonadiabatic interactions. Values of electric fields where $g$ factors of Stark doublets become equal are found. Sharp changes of $g$ factors are observed at the points of avoided crossing of the hyperfine levels.

The dependence of the level's shift due to interaction with $e$EDM and MQM of the $^{177}$Hf nucleus on the rotating electric and magnetic fields for different projections of the total momentum is calculated. The shifts for some levels with small value of projections do not reach saturation up to the magnetic field of 100 G, whereas the levels with the highest projections reach the saturation limit at a very small magnetic field of $\approx 10^{-10 \div -7}$G.

TABLE II. The values $\Delta E_u$ and $\Delta E_l$ (see text for details). $\mathcal{E}_{\text{rot}} = 24$ V/cm in calculations.

| $F_1$ | $F$ | $m_F$ | $\omega$ (kHz) | $\Delta E_l$ (MHz) | $\Delta E_u$ (MHz) |
|---|---|---|---|---|---|
| 9/2 | 5 | 1 | 150 | $6.66243 \times 10^{-2}$ | $6.60901 \times 10^{-2}$ |
| | | | 250 | $1.78572 \times 10^{-1}$ | $1.77226 \times 10^{-1}$ |
| | | 2 | 150 | $1.58640 \times 10^{-4}$ | $1.52535 \times 10^{-4}$ |
| | | | 250 | $1.20935 \times 10^{-3}$ | $1.16315 \times 10^{-3}$ |
| | | 3 | 150 | $1.19590 \times 10^{-7}$ | $1.09330 \times 10^{-7}$ |
| | | | 250 | $2.53924 \times 10^{-6}$ | $2.32070 \times 10^{-6}$ |
| | | 4 | 150 | $3.64828 \times 10^{-11}$ | $6.62874 \times 10^{-11}$ |
| | | | 250 | $2.15341 \times 10^{-9}$ | $3.83477 \times 10^{-9}$ |
| | | 5 | 150 | $4.44089 \times 10^{-15}$ | $7.91900 \times 10^{-12}$ |
| | | | 250 | $6.41265 \times 10^{-13}$ | $2.71951 \times 10^{-9}$ |
| | 4 | 1 | 150 | $3.02679 \times 10^{-2}$ | $3.02678 \times 10^{-2}$ |
| | | | 250 | $8.29207 \times 10^{-2}$ | $8.29175 \times 10^{-2}$ |
| | | 2 | 150 | $2.95556 \times 10^{-5}$ | $2.97533 \times 10^{-5}$ |
| | | | 250 | $2.26799 \times 10^{-4}$ | $2.28309 \times 10^{-4}$ |
| | | 3 | 150 | $8.42976 \times 10^{-9}$ | $8.59549 \times 10^{-9}$ |
| | | | 250 | $1.79483 \times 10^{-7}$ | $1.83383 \times 10^{-7}$ |
| | | 4 | 150 | $1.67590 \times 10^{-11}$ | $7.58504 \times 10^{-13}$ |
| | | | 250 | $1.02960 \times 10^{-9}$ | $4.49258 \times 10^{-11}$ |
| 7/2 | 4 | 1 | 150 | $3.56013 \times 10^{-1}$ | $3.64874 \times 10^{-1}$ |
| | | | 250 | $5.54187 \times 10^{-1}$ | $5.45227 \times 10^{-1}$ |
| | | 2 | 150 | $4.58698 \times 10^{-2}$ | $6.19217 \times 10^{-2}$ |
| | | | 250 | $1.98629 \times 10^{-1}$ | $2.33366 \times 10^{-1}$ |
| | | 3 | 150 | $3.72187 \times 10^{-4}$ | $4.30050 \times 10^{-4}$ |
| | | | 250 | $6.84522 \times 10^{-3}$ | $7.94068 \times 10^{-3}$ |
| | | 4 | 150 | $5.13365 \times 10^{-7}$ | $4.05367 \times 10^{-7}$ |
| | | | 250 | $2.79358 \times 10^{-5}$ | $2.24608 \times 10^{-5}$ |
| | 3 | 1 | 150 | $2.50847 \times 10^{-1}$ | $2.18939 \times 10^{-1}$ |
| | | | 250 | $4.70865 \times 10^{-1}$ | $4.37961 \times 10^{-1}$ |
| | | 2 | 150 | $6.69897 \times 10^{-3}$ | $3.88734 \times 10^{-3}$ |
| | | | 250 | $4.41296 \times 10^{-2}$ | $2.69503 \times 10^{-2}$ |
| | | 3 | 150 | $8.31842 \times 10^{-6}$ | $4.50228 \times 10^{-6}$ |
| | | | 250 | $1.71076 \times 10^{-4}$ | $9.29105 \times 10^{-5}$ |
| 5/2 | 2 | 1 | 150 | $1.88499 \times 10^{-2}$ | $1.99718 \times 10^{-2}$ |
| | | | 250 | $5.18187 \times 10^{-2}$ | $5.48290 \times 10^{-2}$ |
| | | 2 | 150 | $4.02012 \times 10^{-6}$ | $1.92455 \times 10^{-5}$ |
| | | | 250 | $3.09512 \times 10^{-5}$ | $1.50314 \times 10^{-4}$ |
| | 3 | 1 | 150 | $6.73063 \times 10^{-2}$ | $7.06996 \times 10^{-2}$ |
| | | | 250 | $1.74904 \times 10^{-1}$ | $1.85079 \times 10^{-1}$ |
| | | 2 | 150 | $4.03793 \times 10^{-4}$ | $9.53715 \times 10^{-5}$ |
| | | | 250 | $3.07170 \times 10^{-3}$ | $7.29433 \times 10^{-4}$ |
| | | 3 | 150 | $3.12733 \times 10^{-7}$ | $2.11585 \times 10^{-8}$ |
| | | | 250 | $6.26883 \times 10^{-6}$ | $4.50623 \times 10^{-7}$ |

[1] W. B. Cairncross, D. N. Gresh, M. Grau, K. C. Cossel, T. S. Roussy, Y. Ni, Y. Zhou, J. Ye, and E. A. Cornell, Phys. Rev. Lett. **119**, 153001 (2017).

[2] V. V. Flambaum, D. DeMille, and M. G. Kozlov, Phys. Rev. Lett. **113**, 103003 (2014).

[3] A. N. Petrov, L. V. Skripnikov, A. V. Titov, and V. V. Flambaum, Phys. Rev. A **98**, 042502 (2018).

[4] A. N. Petrov, Phys. Rev. A **97**, 052504 (2018).

[5] A. N. Petrov, L. V. Skripnikov, A. V. Titov, N. R. Hutzler, P. W. Hess, B. R. O'Leary, B. Spaun, D. DeMille, G. Gabrielse, and J. M. Doyle, Phys. Rev. A **89**, 062505 (2014).

[6] A. N. Petrov, L. V. Skripnikov, and A. V. Titov, Phys. Rev. A **96**, 022508 (2017).

[7] K. C. Cossel, D. N. Gresh, L. C. Sinclair, T. Coffey, L. V. Skripnikov, A. N. Petrov, N. S. Mosyagin, A. V. Titov, R. W. Field, E. R. Meyer, E. A. Cornell, and J. Ye, Chem. Phys. Lett. **546**, 1 (2012).

[8] N. Stone, At. Data Nucl. Data Tables **90**, 75 (2005).

[9] D. Kunik and U. Kaldor, J. Chem. Phys. **55**, 4127 (1971).

[10] H. J. Monkhorst, Int. J. Quantum Chem. **12**, 421 (1977).

[11] A. N. Petrov, Phys. Rev. A **83**, 024502 (2011).

[12] A. N. Petrov, N. S. Mosyagin, T. A. Isaev, and A. V. Titov, Phys. Rev. A **76**, 030501(R) (2007).

[13] A. N. Petrov, N. S. Mosyagin, and A. V. Titov, Phys. Rev. A **79**, 012505 (2009).

[14] L. V. Skripnikov, J. Chem. Phys. **147**, 021101 (2017).

[15] T. Fleig, Phys. Rev. A **96**, 040502(R) (2017).

[16] L. V. Skripnikov, A. V. Titov, and V. V. Flambaum, Phys. Rev. A **95**, 022512 (2017).

[17] A. Leanhardt, J. Bohn, H. Loh, P. Maletinsky, E. Meyer, L. Sinclair, R. Stutz, and E. Cornell, J. Mol. Spectrosc. **270**, 1 (2011).

[18] D. DeMille, F. B. an S. Bickman, D. Kawall, L. Hunter, D. Krause, Jr., S. Maxwell, and K. Ulmer, AIP Conf. Proc. **596**, 72 (2001).

[19] A. Vutha and D. DeMille, arXiv:0907.5116 (2009).

[20] A. N. Petrov, Phys. Rev. A **91**, 062509 (2015).